In Vivo Positron Emission Tomography (PET) Imaging with an $\alpha_v\beta_6$ Specific Peptide Radiolabeled using [18]F-"Click" Chemistry: Evaluation and Comparison with the Corresponding 4-[[18]F]Fluorobenzoyl- and 2-[[18]F]Fluoropropionyl-Peptides

Sven H. Hausner,† Jan Marik,† M. Karen J. Gagnon, and Julie L. Sutcliffe*

Department of Biomedical Engineering and Center for Molecular and Genomic Imaging, University of California Davis, Davis, California 95616

Received May 21, 2008

Abstract: Numerous radiolabeled peptides have been utilized for in vivo imaging of a variety of cell surface receptors. For applications in PET using [[18]F]fluorine, peptides are radiolabeled via a prosthetic group approach. We previously developed solution-phase [18]F-"click" radiolabeling and solid-phase radiolabeling using 4-[[18]F]fluorobenzoic and 2-[[18]F]fluoropropionic acids. Here we compare the three different radiolabeling approaches and report the effects on PET imaging and pharmacokinetics. The prosthetic groups did have an effect; metabolites with significantly different polarities were observed.

Noninvasive PET[a] imaging has become a widely used tool for the detection of many diseases.[1] Among the available positron emitting nuclides, [[18]F]fluorine is widely used because it can be produced in medical cyclotrons and combines favorable decay-characteristics ($T_{1/2}$ = 110 min; mode of decay: 97% β^+; maximum β^+ energy = 0.64 MeV) with relative chemical versatility.[2] As new disease-specific imaging targets (e.g., cell surface receptors) are being identified, there is an increased demand for targeted radiotracers.[3] Peptides are receiving much attention for in vivo cancer detection because excellent, tissue-specific uptake can be achieved. Relying on well-established synthetic chemistries, peptides are readily produced and modified.[3] Strategies include automated syntheses with incorporation of unnatural amino acids, peptidomimetics, and cyclization, among others, to develop compounds with desirable pharmacokinetic properties. To make peptides amendable for PET imaging, the [[18]F]fluorine-radiolabel is introduced using small molecules (prosthetic groups). Examples of [[18]F]-labeled peptides for PET imaging include octreotide,[4] vasoactive intestinal peptide,[5] integrin specific peptides,[6−8] N^ε-(γ-glutamyl)lysine,[9] neurotensin analogues,[10] human C-peptide,[11] and insulin.[12]

The prosthetic group approach involves at least two synthetic steps: incorporation of [[18]F]fluorine into the prosthetic group and attachment to the peptide. Generally, the prosthetic group itself should not negatively affect receptor binding, and the synthetic approach should be applicable to many different peptide substrates with minimal synthetic modifications. For this, fast, simple chemistries amendable to automation are desirable.[13] Many different strategies have been explored in recent years.[2] Widely used approaches include the conjugation to free amino groups on the peptide in solution using [18]F-radiolabeled acids such as 4-[[18]F]fluorobenzoic ([[18]F]FBA) acid and 2-[[18]F]fluoropropionic ([[18]F]FPA) acid or their activated forms, *N*-succinimidyl-4-[[18]F]fluorobenzoate ([[18]F]SFB) and *p*-nitrophenyl 2-[[18]F]fluoropropionate ([[18]F]NFP), respectively. The successful use of activated esters is limited to peptides bearing only one free amino group, as otherwise a complex mixture of radiolabeled products is obtained. Also, the low stability of [[18]F]SFB in solutions at a pH required for the conjugation has been found as a limiting factor in this approach.[14] The conjugation of [[18]F]FBA and [[18]F]FPA to the selectively deprotected peptide attached to a solid support has been developed to overcome the above-mentioned drawbacks.[15,16] In the solid-phase approach, the peptide is assembled on a solid support and only the amino group for the attachment of [[18]F]FBA or [[18]F]FPA is selectively deprotected. The prosthetic group is then conjugated to the peptide using in situ activation, followed by simultaneous cleavage of the radiolabeled peptide from the solid support and complete side chain deprotection (Table 1, Scheme 1).

For cases where radiolabeling on solid phase is not possible or advantageous, such as preparations involving certain post-

Table 1. Radiotracers Prepared[a]

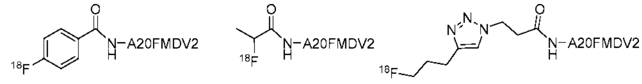

1 2 3

compd	Rxn steps[b]	type	group	synthesis time[c]	radio-HPLC purity	yield[d]
1	4	solid phase	[[18]F]FBA	137 min	>99%	7.8 ± 2.2%
2	4	solid phase	[[18]F]FPA	171 min	>99%	4.6 ± 0.8%
3	2	solution	[[18]F]FC5	66 min	>98%	8.7 ± 2.3%

[a] A20FMDV2 = NAVPNLRGDLQVLAQKVART-C(O)NH_2. [b] Preparation of radiotracer starting from $K^{18}F$ and the selectively deprotected peptide. [c] Since EOB. [d] Decay corrected radiochemical yield based on amount of $K^{18}F$ at EOB.

Scheme 1. Radiosyntheses of Imaging Tracers Evaluated[a]

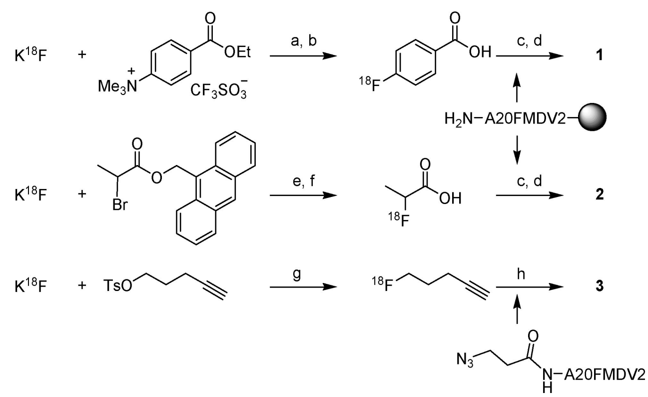

[a] Reagents and conditions: (a) K222, DMSO/acetonitrile, 100 °C. (b) (i) NaOH, 100 °C; (ii) HCl, (iii) C18 Sep-Pak. (c) HATU, DIEA, DMF. (d) (i) TFA/TIPS/H_2O; (ii) HPLC. (e) (i) K222, acetonitrile, 100 °C; (ii) HPLC. (f) TEA, DMF/acetonitrile/H_2O, 100 °C. (g) Acetonitrile, 100 °C. (h) (i) CuI, Na ascorbate, DIEA, DMF/acetonitrile/H_2O, room temperature; (ii) HPLC.

* To whom correspondence should be addressed. Phone: 530-754-7107. Fax: 530-754-5739. E-mail: jlsutcliffe@ucdavis.edu.

† Contributed equally.

[a] Abbreviations: β^+, positron; DIEA, diisopropylethylamine; DMF, *N*,*N*-dimethylformamide; DMSO, dimethylsulfoxide; EOB, end of bombardment; K222, Kryptofix 222; PET, positron emission tomography; p.i., post injection; R_t, retention time; $T_{1/2}$, half-life; TEA, triethylamine; TFA, 2,2,2-trifluoroacetic acid; TIPS, triisopropylsilane; % ID/g, percent of injected radioactive dose per gram of tissue.

10.1021/jm800608s CCC: $40.75
Published on Web 09/12/2008

cleavage modifications (e.g., introduction of acid sensitive groups, certain cyclizations) or workups requiring time-consuming purification procedures, several mild, chemoselective methods have been developed to attach the radiolabeled prosthetic group to unprotected peptides in solution (e.g., 4-[^{18}F]fluorobenzaldehyde to an aminooxyacetic acid or a 6-hydrazinonicotinic acid group;[17,18] [^{18}F]fluorothiols to a chloroacetic acid group[19]). All chemoselective conjugations of prosthetic groups require modification of the peptide with a functional group that can provide a chemistry orthogonal to all other functional groups found in the peptide.

Recently, our group successfully used the copper-catalyzed Huisgen 1,3-dipolar cycloaddition ("click" chemistry)[20,21] to conjugate ω-[^{18}F]fluoroalkynes to peptides functionalized with 3-azidopropionic acid (Table 1, Scheme 1).[22] The formation of 1,4-disubstituted 1,2,3-triazoles proceeded smoothly under mild conditions, and the radiolabeled peptides were obtained in a short period of time. Subsequently, this approach has been applied for radiolabeling of different substrates with [^{18}F]-fluorine.[10,23−25] As a result of ongoing improvements in 1,3-dipolar cycloaddition chemistry and because of its versatility and short reaction times, "click" radiochemistry promises to become a widely used tool for preparation of radiotracers.

Here we present an evaluation of the feasibility of in vivo imaging with a [^{18}F]-labeled "click" probe. A20FMDV2, a peptide that selectively binds to the integrin $\alpha_v\beta_6$, was chosen as model peptide (Table 1).[8,26] Expression of the epithelial-specific integrin $\alpha_v\beta_6$ is tightly regulated. It is low or undetectable in adult tissues but has been shown to be increased in many different cancers, including colon, cervical, lung, and pancreatic cancer; the integrin $\alpha_v\beta_6$ has also been described as a prognostic biomarker linked to poor survival.[27−31] We have shown recently in a mouse model that [^{18}F]FBA-A20FDMV2 (**1**) can be used to selectively image $\alpha_v\beta_6$-expressing tumors.[8]

The same mouse model, male athymic nude mice bearing $\alpha_v\beta_6$-positive (DX3puroβ6) and $\alpha_v\beta_6$-negative (DX3puro, control) cell xenografts, was employed here for comparison of [^{18}F]FBA-A20FDMV2 (**1**), [^{18}F]FPA-A20FDMV2 (**2**), and [^{18}F]FC5-A20FDMV2 (**3**) (Supporting Information). Data presented compare tracer preparation, microPET imaging, biodistribution, and an initial metabolic evaluation.

As mentioned above, compounds **1** and **2** were prepared by solid-phase radiolabeling, while the chemoselective "click" approach was chosen to prepare **3** from 5-[^{18}F]fluoro-1-pentyne and *N*-(3-azidopropionyl)-A20FMDV2 (Scheme 1). All prosthetic groups were attached to the N-terminal amino group of the peptide chain. Their different chemical nature changed the chemical properties of the radiotracer, that is size, lipophilicity, and ability to form hydrogen bonds. The smallest prosthetic group used was [^{18}F]FPA; it has to be noted that this prosthetic group is obtained as a mixture of enantiomers and therefore the final radiolabeled peptide **2** was a mixture of diastereoisomers. The medium sized [^{18}F]FBA was expected to provide the final product **1** with increased lipophilicity. Within the set of prosthetic groups evaluated, the 1,4 disubstituted 1,2,3-triazole ([^{18}F]FC5) in tracer **3** was the largest. However, the large dipole moment and the ability of the nitrogen atoms in positions one and three of the triazole ring to form hydrogen bonds decreased the lipophilicity of the final radiolabeled peptide. The reversed-phase HPLC retention times for the three compounds corroborated these assumptions (**1** 16.6 min, **2** 14.7 min, and **3** 14.7 min; Supporting Information Figure S1).

Several details are worth noting when comparing the three radiolabeling procedures summarized in Table 1. First, while labeling with [^{18}F]FBA[13] and [^{18}F]FPA[16,32] followed similar procedures, the preparation of **2** required an additional 34 min owing to the required HPLC purification of the 9-methylanthranyl 2-[^{18}F]fluoropropionate intermediate. Second, when preparing [^{18}F]FBA and [^{18}F]FPA for coupling, DMF (50 μL) was added to the final solution of the [^{18}F]FBA or [^{18}F]FPA to minimize evaporative loss during removal of the acetonitrile used as solvent during the preparation. A very gentle stream of nitrogen (100 cm^3/min) and heating to not more than 100 °C were applied, as more vigorous conditions led to substantial loss of [^{18}F]FBA or [^{18}F]FPA. Addition of 5−10 μg of *N,N,N,N*-tetramethylammonium hydroxide, commonly used to prevent evaporative loss, negatively affected the yield of the subsequent coupling reaction. For coupling to the peptide, the prosthetic group (in 50 μL DMF) was withdrawn to a 1 mL fritted syringe containing the preswollen resin, followed by the coupling reagent (HATU in 30 μL DMF) and the base (DIEA in 30 μL DMF). The order of addition of the regents has been found to be crucial for the success of the coupling. The optimal amount of the resin was 5 mg. Lower amounts led to lower yields, while higher amounts did not significantly improve the yields.

When comparing the solid-phase radiolabeling of A20FMDV2 to radiolabeling of other substrates, it was found that the yields of the coupling reactions depended mostly on the size and complexity of the peptide. They were 22 ± 4% (n = 5) and 13 ± 3% (n = 3) for coupling of [^{18}F]FBA or [^{18}F]FPA, respectively, to the 20 amino acid peptide A20FMDV2. By comparison, coupling yields for [^{18}F]FBA to octapeptides averaged over 50% but dropped to about 15% for peptides containing over 50 amino acids. The yields for [^{18}F]FPA conjugation were slightly lower than those for [^{18}F]FBA. For both prosthetic groups, the yields of TFA-mediated cleavage of the final product from the solid support and the simultaneous removal of the side chain protecting groups were 71 ± 4% (n = 8).

"Click" radiolabeling, like any generally applicable chemoselective conjugation of a prosthetic group to an unprotected peptide, requires modification of the peptide before the conjugation can be performed. Here, the 3-azidopropionyl group was introduced at the N-terminus of A20FMDV2 for the conjugation of 5-[^{18}F]fluoro-1-pentyne. Again, in general, the yield of the Cu^{I} catalyzed conjugation depended on the size and complexity of the peptide substrate. Short peptides provided near quantitative yields,[22] but longer peptides like A20FMDV2 were obtained in yields below 10% and required approximately 1 mg of peptide precursor.

In all three cases, the radiolabeled peptides were easily separated from nonradiolabeled peptide precursors using HPLC based on the difference in polarities caused by introduction of the prosthetic groups (Supporting Information Figure S1). Remaining amounts of unreacted [^{18}F]FBA and [^{18}F]FPA were washed away from the solid support before cleavage of the peptide from the solid support, while unreacted 5-[^{18}F]fluoro-1-pentyne was evaporated during the drying step. All three ^{18}F-fluoropeptides were characterized by coelution with nonradioactive standards. The specific activities of purified final products were >37 GBq/μmol based on HPLC analysis.

Overall, the total yields of the radiolabeled products obtained from solid-phase and chemoselective "click" approaches were comparable but several significant differences were observed. Although the "click" approach provided the product in less than half of the time needed for the solid-phase syntheses and in only two radiochemical steps, the solid-phase approaches required smaller amounts of the starting material; "click"

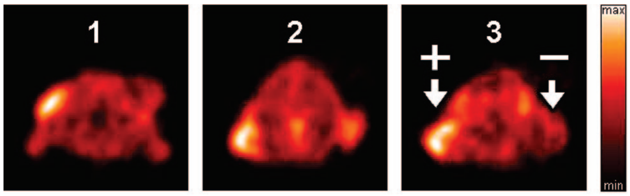

Figure 1. Representative normalized transaxial sections of microPET scans (60−75 min p.i.) with compounds **1**, **2**, and **3** in mice bearing paired human cell xenografts ($\alpha_v\beta_6$-expressing DX3puroβ6, and $\alpha_v\beta_6$-negative parent DX3puro).

conjugation required 1 mg of purified *N*-(3-azidopropionyl)-A20FMDV2 versus 5 mg of resin (bearing the crude peptide) for the solid-phase syntheses. Also, the solid-phase approach is more easily amendable for automation of the radiochemical procedure. In general, the chemoselective "click" method is faster but the solid-phase approach seems to be more versatile and cost-effective for peptides such as A20FMDV2. Thus, at least for the moment, the chemoselective "click" approach appears to be more suitable for short peptides (or those requiring time-consuming postcleavage procedures) and small molecules, while the solid-phase approach appears more advantageous for long peptide chains.

For evaluation of the effects of the prosthetic groups on pharmacokinetics, microPET and biodistribution studies were carried out with tracers **1**−**3** in athymic nude mice bearing paired human xenografts ($\alpha_v\beta_6$-positive, and $\alpha_v\beta_6$-negative control).[8] MicroPET imaging data were acquired as dynamic 4 × 15 min scans (n = 3/tracer), beginning 15 min after injection. As depicted in Figure 1, all three tracers were able to target the $\alpha_v\beta_6$-positive DX3puroβ6 tumor. Tracers **1** and **3** showed better DX3puroβ6/DX3puro and DX3puroβ6/background ratios than **2**. Overall, the PET data paralleled the biodistribution data, showing highest levels of activity in kidneys and the urinary bladder (Supporting Information Figure S2). Thus, the radiotracer **3** prepared by "click" chemistry can be considered comparable to other radiotracers bearing established prosthetic groups, yielding images similar to those of the [^{18}F]FBA-tracer **1**.

Biodistribution studies revealed generally similar uptake-patterns of **1**−**3** for most organs and the tumors (n = 3/tracer, 1 h p.i., Chart 1, Supporting Information Table S1). Renal clearance was the dominant route of elimination, with **1** resulting in highest levels of activity in the urine (**1** 1082 ± 279% ID/g, **2** 311 ± 133% ID/g, **3** 501 ± 332% ID/g), while **3** appeared to result in moderately increased levels of radioactivity in the kidneys and the liver.

Uptake levels in the $\alpha_v\beta_6$-positive tumor 1 h after injection were 0.66 ± 0.09% ID/g, 1.18 ± 0.28% ID/g, and 1.01 ± 0.09% ID/g for **1**, **2**, and **3**, respectively. While **2** showed the highest uptake, the $\alpha_v\beta_6$-positive/$\alpha_v\beta_6$-negative tumor uptake ratio was comparatively low (1.9:1 vs > 3:1 for **1** and **3**, Table 2). A similar trend was found for the $\alpha_v\beta_6$-positive tumor/blood ratio. These differences are noteworthy, as they demonstrate the effect of the prosthetic groups on tumor-targeting and pharmacokinetics. The results are even more surprising in light of the identical HPLC-retention times of **2** and **3**. Furthermore, **1** had the longest HPLC-retention time (highest lipophilicity), which would be expected to favor liver uptake, yet it resulted in highest levels of radioactivity in the urine.

A possible answer to this may lie in the metabolic fate of the compounds. As stated above, renal clearance was the main route of excretion for all three tracers. When urine samples taken 1 h p.i. were analyzed by radio-HPLC, none of them contained

Chart 1. Biodistribution of Tracers **1**−**3** in Male Athymic Nude Mice 1 h after Injection (n = 3/tracer)[a]

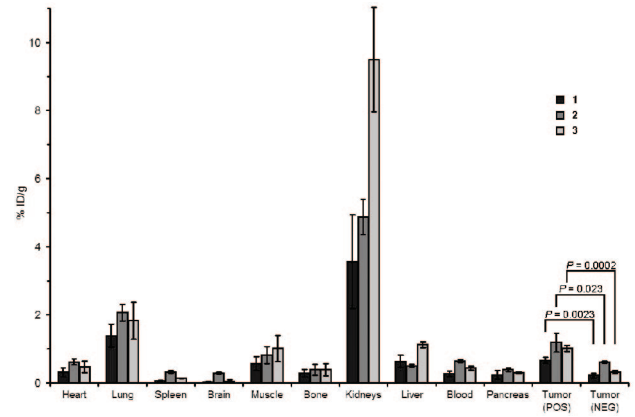

[a] Levels of radioactivity in healthy tissues, as well as $\alpha_v\beta_6$-positive (DX3puroβ6) and $\alpha_v\beta_6$-negative (DX3puro) tumors are expressed as % ID/g. Data for **1** were taken from ref 8.

Table 2. Uptake Ratios for Tumors and Selected Organs[a]

compd	DX3puroβ6/DX3puro[b]	DX3puroβ6/blood	DX3puroβ6/kidneys
1	3.1:1	2.5:1[c]	1:5.4[d]
2	1.9:1	1.8:1[d]	1:4.1[e]
3	3.3:1	2.3:1[e]	1:9.4[e]

[a] Based on biodistribution (1 h p.i.). [b] For P-values, see Chart 1. [c] $P < 0.01$. [d] $P < 0.05$. [e] $P < 0.001$.

unmetabolized radiotracer (Supporting Information Figure S3). Instead, three radioactive metabolites were observed for **1** (R_t = 9.0, 10.4, 10.8 min vs R_t(**1**) = 16.6 min), while **2** yielded two metabolites with very short retention times (i.e., high hydrophilicities; R_t = 2.1, 3.2 min vs R_t(**2**) = 14.7 min). Similarly, two main metabolites with intermediate retention times were detected for **3** (R_t = 5.9, 8.6 min vs R_t(**3**) = 14.7 min). This initial analysis indicated that, despite identical peptide sequence and comparable overall biodistribution, significant pharmacokinetic differences do exist and that they have to be attributed to the prosthetic groups. It can be assumed that the (comparatively minor) differences in % ID/g-values between **1**, **2**, and **3** seen for individual organs can be linked at least partially to different excretion characteristics of the metabolites as well. The differences would likely have been more pronounced were it not for the fact that all the metabolites examined here were more hydrophilic (i.e., had shorter HPLC retention times) than the intact tracers, resulting in rapid renal excretion. However, such a favorable clearance behavior can not necessarily be expected for metabolites of other tracers.

In conclusion, we compared three ^{18}F-prosthetic groups, [^{18}F]FBA, [^{18}F]FPA, and [^{18}F]FC5, the latter introduced by "click" chemistry, for peptide radiolabeling and in vivo studies. All three prosthetic groups were readily introduced at the N-terminus of a tumor targeting model peptide with similar overall radiolabeling yields. The "click" radiolabeling approach was fastest but required a relatively large amount of purified peptide precursor. During in vivo animal studies, we observed that the prosthetic groups had a noticeable effect on pharmacokinetics, notably tumor uptake and metabolic fate, thus underscoring the necessity for the investigation of different prosthetic groups that allow combination of convenient chemistries with favorable pharmacokinetics for each individual tracer under development.

Acknowledgment. We thank David L. Kukis, Salma Jivan, Craig Abbey, John F. Marshall, Catherine E. Stanecki, and Julia Choi. This work was supported by NIH grant no. R21 CA107792.

Supporting Information Available: Experimental details and analytical data for precursors, nonradioactive analogues and radiotracers, and information about the imaging studies. This material is available free of charge via the Internet at http://pubs.acs.org.

References

(1) Cherry, S. R. The 2006 Henry N. Wagner lecture: Of mice and men (and positrons): advances in PET imaging technology. *J. Nucl. Med.* **2006**, *47*, 1735–1745.

(2) Schirrmacher, R.; Wängler, C.; Schirrmacher, E. Recent developments and trends in ^{18}F-radiochemistry: syntheses and applications. *Mini Rev. Org. Chem.* **2007**, *4*, 317–329.

(3) Okarvi, S. M. Peptide-based radiopharmaceuticals: Future tools for diagnostic imaging of cancers and other diseases. *Med. Res. Rev.* **2004**, *24*, 357–397.

(4) Guhlke, S.; Wester, H. J.; Bruns, C.; Stöcklin, G. (2-[^{18}F]Fluoropropionyl-(D)Phe^{1})-Octreotide, a potential radiopharmaceutical for quantitative somatostatin receptor imaging with PET: synthesis, radiolabeling, in vitro validation and biodistribution in mice. *Nucl. Med. Biol.* **1994**, *21*, 819–825.

(5) Jagoda, E. M.; Aloj, L.; Seidel, J.; Lang, L.; Moody, T. W.; Green, S.; Caraco, C.; Daube-Witherspoon, M.; Green, M. V.; Eckelman, W. C. Comparison of an ^{18}F labeled derivative of vasoactive intestinal peptide and 2-deoxy-2-[^{18}F]fluoro-D-glucose in nude mice bearing breast cancer xenografts. *Mol. Imaging Biol.* **2002**, *4*, 369–379.

(6) Haubner, R.; Kuhnast, B.; Mang, C.; Weber, W. A.; Kessler, H.; Wester, H. J.; Schwaiger, M. [^{18}F]Galacto-RGD: Synthesis, radiolabeling, metabolic stability, and radiation dose estimates. *Bioconjugate Chem.* **2004**, *15*, 61–69.

(7) Chen, X. Y.; Park, R.; Shahinian, A. H.; Tohme, M.; Khankaldyyan, V.; Bozorgzadeh, M. H.; Bading, J. R.; Moats, R.; Laug, W. E.; Conti, P. S. ^{18}F-labeled RGD peptide: initial evaluation for imaging brain tumor angiogenesis. *Nucl. Med. Biol.* **2004**, *31*, 179–189.

(8) Hausner, S. H.; DiCara, D.; Marik, J.; Marshall, J. F.; Sutcliffe, J. L. Use of a peptide derived from foot-and-mouth disease virus for the noninvasive imaging of human cancer: generation and evaluation of 4-[^{18}F]fluorobenzoyl A20FMDV2 for in vivo imaging of integrin $\alpha_v\beta_6$ expression with positron emission tomography. *Cancer Res.* **2007**, *67*, 7833–7840.

(9) Wüst, F.; Hultsch, C.; Bergmann, R.; Johannsen, B.; Henle, T. Radiolabelling of isopeptide N$^{\varepsilon}$-(γ-glutamyl)-L-lysine by conjugation with *N*-succinimidyl-4-[^{18}F]fluorobenzoate. *Appl. Radiat. Isot.* **2003**, *59*, 43–48.

(10) Ramenda, T.; Bergmann, R.; Wuest, F. Synthesis of ^{18}F-labeled neurotensin(8−13) via copper-mediated 1,3-dipolar [3 + 2] cycloaddition reaction. *Lett. Drug Des. Discovery* **2007**, *4*, 279–285.

(11) Fredriksson, A.; Johnström, P.; Stone-Elander, S.; Jonasson, P.; Nygren, P. A.; Ekberg, K.; Johansson, B. L.; Wahren, J. Labeling of human C-peptide by conjugation with *N*-succinimidyl-4-[^{18}F]fluorobenzoate. *J. Labelled Comp. Rad.* **2001**, *44*, 509–519.

(12) Shai, Y.; Kirk, K. L.; Channing, M. A.; Dunn, B. B.; Lesniak, M. A.; Eastman, R. C.; Finn, R. D.; Roth, J.; Jacobson, K. A. ^{18}F-Labeled insulin: A prosthetic group methodology for incorporation of a positron emitter into peptides and proteins. *Biochemistry* **1989**, *28*, 4801–4806.

(13) Marik, J.; Sutcliffe, J. L. Fully automated preparation of n.c.a. 4-[^{18}F]fluorobenzoic acid and *N*-succinimidyl 4-[^{18}F]fluorobenzoate using a Siemens/CTI chemistry process control unit (CPCU). *Appl. Radiat. Isot.* **2007**, *65*, 199–203.

(14) Li, J.; Trent, J. O.; Bates, P. J.; Ng, C. K. Labeling G-rich oligonucleotides (GROs) with *N*-succinimidyl 4-[^{18}F]fluorobenzoate (S^{18}FB). *J. Labelled Compd. Radiopharm.* **2006**, *49*, 1213–1221.

(15) Sutcliffe-Goulden, J. L.; O'Doherty, M. J.; Marsden, P. K.; Hart, I. R.; Marshall, J. F.; Bansal, S. S. Rapid solid phase synthesis and biodistribution of ^{18}F-labelled linear peptides. *Eur. J. Nucl. Med. Mol. Imaging* **2002**, *29*, 754–759.

(16) Marik, J.; Hausner, S. H.; Fix, L. A.; Gagnon, M. K. J.; Sutcliffe, J. L. Solid-phase synthesis of 2-[^{18}F]fluoropropionyl peptides. *Bioconjugate Chem.* **2006**, *17*, 1017–1021.

(17) Poethko, T.; Schottelius, M.; Thumshirn, G.; Hersel, U.; Herz, M.; Henriksen, G.; Kessler, H.; Schwaiger, M.; Wester, H. J. Two-step methodology for high-yield routine radiohalogenation of peptides: ^{18}F-labeled RGD and octreotide analogs. *J. Nucl. Med.* **2004**, *45*, 892–902.

(18) Bruus-Jensen, K.; Poethko, T.; Schottelius, M.; Hauser, A.; Schwaiger, M.; Wester, H. J. Chemoselective hydrazone formation between HYNIC-functionalized peptides and ^{18}F-fluorinated aldehydes. *Nucl. Med. Biol.* **2006**, *33*, 173–183.

(19) Glaser, M.; Karlsen, H.; Solbakken, M.; Arukwe, J.; Brady, F.; Luthra, S. K.; Cuthbertson, A. ^{18}F-fluorothiols: a new approach to label peptides chemoselectively as potential tracers for positron emission tomography. *Bioconjugate Chem.* **2004**, *15*, 1447–1453.

(20) Kolb, H. C.; Finn, M. G.; Sharpless, K. B. Click chemistry: diverse chemical function from a few good reactions. *Angew. Chem., Int. Ed.* **2001**, *40*, 2004–2021.

(21) Kolb, H. C.; Sharpless, K. B. The growing impact of click chemistry on drug discovery. *Drug Discovery Today* **2003**, *8*, 1128–1137.

(22) Marik, J.; Sutcliffe, J. L. Click for PET: rapid preparation of [^{18}F]fluoropeptides using Cu^{I} catalyzed 1,3-dipolar cycloaddition. *Tetrahedron Lett.* **2006**, *47*, 6681–6684.

(23) Glaser, M.; Årstad, E. "Click labeling" with 2-[^{18}F]fluoroethylazide for positron emission tomography. *Bioconjugate Chem.* **2007**, *18*, 989–993.

(24) Sirion, U.; Kim, H. J.; Lee, J. H.; Seo, J. W.; Lee, B. S.; Lee, S. J.; Oh, S. J.; Chi, D. Y. An efficient F-18 labeling method for PET study: Huisgen 1,3-dipolar cycloaddition of bioactive substances and F-18-labeled compounds. *Tetrahedron Lett.* **2007**, *48*, 3953–3957.

(25) Li, Z. B.; Wu, Z.; Chen, K.; Chin, F. T.; Chen, X. Click chemistry for ^{18}F-labeling of RGD peptides and microPET imaging of tumor integrin $\alpha_v\beta_3$ expression. *Bioconjugate Chem.* **2007**, *18*, 1987–1994.

(26) DiCara, D.; Rapisarda, C.; Sutcliffe, J. L.; Violette, S. M.; Weinreb, P. H.; Hart, I. R.; Howard, M. J.; Marshall, J. F. Structure−function analysis of Arg-Gly-Asp helix motifs in $\alpha_v\beta_6$ integrin ligands. *J. Biol. Chem.* **2007**, *282*, 9657–9665.

(27) Sheppard, D.; Rozzo, C.; Starr, L.; Quaranta, V.; Erle, D. J.; Pytela, R. Complete amino acid sequence of a novel integrin β subunit (β_6) identified in epithelial cells using the polymerase chain reaction. *J. Biol. Chem.* **1990**, *265*, 11502–11507.

(28) Elayadi, A. N.; Samli, K. N.; Prudkin, L.; Liu, Y. H.; Bian, A. H.; Xie, X. J.; Wistuba, I. I.; Roth, J. A.; McGuire, M. J.; Brown, K. C. A peptide selected by biopanning identifies the integrin $\alpha_v\beta_6$ as a prognostic biomarker for nonsmall cell lung cancer. *Cancer Res.* **2007**, *67*, 5889–5895.

(29) Bates, R. C.; Bellovin, D. I.; Brown, C.; Maynard, E.; Wu, B. Y.; Kawakatsu, H.; Sheppard, D.; Oettgen, P.; Mercurio, A. M. Transcriptional activation of integrin β_6 during the epithelial−mesenchymal transition defines a novel prognostic indicator of aggressive colon carcinoma. *J. Clin. Invest.* **2005**, *115*, 339–347.

(30) Hazelbag, S.; Kenter, G. G.; Gorter, A.; Dreef, E. J.; Koopman, L. A.; Violette, S. M.; Weinreb, P. H.; Fleuren, G. J. Overexpression of the $\alpha_v\beta_6$ integrin in cervical squamous cell carcinoma is a prognostic factor for decreased survival. *J. Pathol.* **2007**, *212*, 316–324.

(31) Koopman Van Aarsen, L. A.; Leone, D. R.; Ho, S.; Dolinski, B. M.; McCoon, P. E.; LePage, D. J.; Kelly, R.; Heaney, G.; Rayhorn, P.; Reid, C.; Simon, K. J.; Horan, G. S.; Tao, N.; Gardner, H. A.; Skelly, M. M.; Gown, A. M.; Thomas, G. J.; Weinreb, P. H.; Fawell, S. E.; Violette, S. M. Antibody-mediated blockade of integrin $\alpha_v\beta_6$ inhibits tumor progression in vivo by a transforming growth factor-β-regulated mechanism. *Cancer Res.* **2008**, *68*, 561–570.

(32) Wester, H. J.; Hamacher, K.; Stöcklin, G. A comparative study of NCA fluorine-18 labeling of proteins via acylation and photochemical conjugation. *Nucl. Med. Biol.* **1996**, *23*, 365–372.

JM800608S